

See discussions, stats, and author profiles for this publication at: <https://www.researchgate.net/publication/46819098>

Magnetically Powered Flexible Metal Nanowire Motors

ARTICLE in JOURNAL OF THE AMERICAN CHEMICAL SOCIETY · SEPTEMBER 2010

Impact Factor: 12.11 · DOI: 10.1021/ja1072349 · Source: PubMed

CITATIONS

107

READS

152

5 AUTHORS, INCLUDING:



[Wei Gao](#)

University of California, Berkeley

59 PUBLICATIONS 1,797 CITATIONS

SEE PROFILE



[Sirilak Sattayasamitsathit](#)

University of California, San Diego

43 PUBLICATIONS 1,287 CITATIONS

SEE PROFILE



[Daniel Weihs](#)

Technion - Israel Institute of Technology

169 PUBLICATIONS 3,469 CITATIONS

SEE PROFILE

Magnetically Powered Flexible Metal Nanowire Motors

Wei Gao,[†] Sirilak Sattayasamitsathit,[†] Kalayil Manian Manesh,[†] Daniel Weihs,[‡] and Joseph Wang^{*,†}

Department of Nanoengineering, University of California San Diego, La Jolla, California 92093, and Faculty of Aerospace Engineering, Technion, Haifa, 32000, Israel

Received August 11, 2010; E-mail: josephwang@ucsd.edu

Abstract: Fuel-free magnetically driven propulsion of flexible Au/Ag/Ni nanowires, with a gold ‘head’ and nickel ‘tail’, linked by a partially dissolved and weakened silver bridge, is described. The flexible bridge facilitates the cyclic mechanical deformations under an external rotating magnetic field. Under such a field the nickel segment starts to rotate, facilitating the rotation of the gold segment at a different amplitude, hence breaking the system symmetry and inducing the movement. Forward (‘pushing’) and backward (‘pulling’) magnetically powered locomotion and a precise On/Off motion control are achieved by tailoring the length of the nickel and gold segments and modulating the magnetic field, respectively. Efficient locomotion in urine samples and in high-salt media is illustrated. The new magnetic nanowire swimmers can be prepared in large scale using a simple template electrodeposition protocol and offer considerable promise for diverse practical applications.

The use of nanomotors to power nanomachines and nanofactories is currently a research area of intense activity due to numerous potential applications.¹ Most attention in the development of artificial nanomotors has been given to catalytic nanowire motors that exhibit autonomous self-propulsion in the presence of a hydrogen peroxide fuel.¹ However, numerous potential applications of future nanomachines, particularly biomedical ones, would require elimination of the fuel requirements. Efforts in this direction have recently led to the propulsion of fuel-free nanowire diodes under external electric fields.²

Magnetically controlled motion, inspired by the motility of prokaryotic and eukaryotic microorganisms,³ represents another attractive route for addressing the challenge of nanoscale propulsion and accomplishing a fuel-free locomotion. Such nanoscale propulsion requires breaking the system symmetry by deforming the motor shape.⁴ For example, *E. coli* bacteria use rotating helical flagella to propel in viscous media.^{3b} Magnetic force has been widely used to provide the mechanical deformation essential for breaking the symmetry. The controlled beating motion of flexible DNA-linked assemblies of paramagnetic microparticles was illustrated by Dreyfus et al.⁵ Nelson⁶ and Ghosh⁷ reported recently the fabrication and magnetically controlled motion of efficient artificial flagella consisting of helical tails. These cork-screw swimmers offer attractive propulsion but require specialized ‘top down’ self-scroll or shadow-growth preparation routes along with advanced microfabrication facilities.

Here we demonstrate a simple new approach for addressing the fuel requirement and for creating magnetically driven propulsion based on easily prepared flexible metal nanowire swimmers. As illustrated in SI Scheme 1A, the new three-segment nanowire motors (~6 μm long, 200 nm in diameter) are readily prepared using a template electrodeposition approach. Such preparation involves the sequential

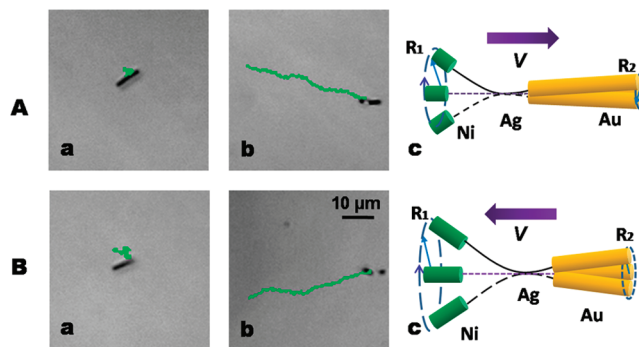
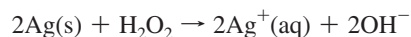


Figure 1. Comparison of the ‘forward’ (A) and ‘backward’ (B) movement of rigid Au/Ag/Ni (a) and flexible Au/Ag_{flex}/Ni (b) nanowires under a rotating magnetic field (5 G, $f = 15$ (A); 10 (B) Hz) over a 15 s period. The lengths of the Au, Ag, and Ni segments are as follows: (A) 3, 3, and 0.5 μm; (B) 2, 3.5, and 1 μm, respectively. (See corresponding SI Video 2 and SI Figure 1) (c) Schematic of the magnetic swimmer moving ‘forward’ (A) and ‘backward’ (B).

deposition of the Au, Ag, and Ni segments into the alumina membrane micropores. Subsequent dissolution of the template and release of the nanowires are followed by partial dissolution of the central silver segment in hydrogen peroxide to create the flexible thinner joint (linking the Au ‘head’ and Ni ‘tail’) essential for the controlled mechanical deformation. The flexibility of thin Ag nanowires has been discussed earlier.⁸ Flexible nanorods based on a polyelectrolyte bridge were also described by Ozin’s team but not in connection to directed motion.⁹ The new template electrochemical synthesis of flexible metal nanowires greatly simplifies the preparation of magnetic swimmers compared to the fabrication of cork-screw or helical magnetic propellers^{6,7} and offers reproducible preparation that reflects the precise charge control. The resulting fuel-free flexible nanowire swimmers offer great promise for diverse biomedical applications as indicated below from their efficient propulsion in urine medium.

SI Video 1 clearly illustrates the rapid and yet incomplete dissolution of the central Ag segment and formation of a flexible joint within 10–15 s in the peroxide solution. A SEM image of the resulting flexible Ag section (SI Figure 2) indicates a rough porous segment of a slightly smaller diameter compared to its nonporous metal neighbors. The dissolution of silver in hydrogen peroxide



leads to hydroxyl products that chemisorb on the Ag surface and results in AgOH and Ag₂O surface products.^{10,11} Such formation of surface byproducts in the presence of hydrogen peroxide has been shown to hinder further silver dissolution.^{10,11}

To illustrate the critical role of the nanowire flexibility in achieving the magnetic propulsion we compared the motion of Au/Ag/Ni nanowires before and after the partial silver dissolution. Figure 1A displays the motion trajectories of conventional Au/Ag/Ni nanowires

[†] University of California San Diego.

[‡] Technion.

(a) and flexible Au/Ag_{flex}/Ni (b) over a 15 s period, taken from videos of the nanowires under the rotating magnetic field (SI Video 2). The flexible nanowire exhibits defined locomotion over a dramatically long path, parallel to the magnetic field axis (b), with a cone-shaped rotation of the Ni 'tail' (shown in SI Video 2). The speed of this nanomotor is $\sim 3 \mu\text{m s}^{-1}$, i.e., approximately 0.5 body length s^{-1} . In contrast, no directed motion is observed for the control experiment involving the rigid Au/Ag/Ni nanowires over the same time period (a).

To actuate the locomotion in a nonreciprocal fashion at low Reynolds number, artificial swimming devices deform their shape. The observed locomotion of the nanowire swimmer is attributed to the transfer of the magnetic energy into cyclic mechanical deformations. The flexible Ag bridge is essential for generating such cyclic mechanical deformations under an external rotating magnetic field (SI Scheme 1B). SI Video 2 clearly demonstrates the rotation of the Ni 'tail' that resembles the rotation mechanism of microorganisms. Similar to natural microorganisms, our artificial nanowire swimmers consist of a body and a propulsive appendage, deforming in a continuous fashion. The rotating magnetic field creates a cone-shaped rotation of the Ni segment which causes rotation of the Au segment on the opposite end. Such rotation of Au and Ni segments with different amplitudes and phase difference, due to bending of the Ag joint, breaks the system symmetry to induce the movement (Figure 1c). Propulsion is achieved when the flexibility of the connecting thin Ag wire allows for bending, so that the shorter Ni segment, which has larger amplitude, is tilted backward relative to the cone surface. Thus, when rotated, this section produces a force away from the centroid of the swimmer. The flexibility of the central Ag bridge facilitates generation of rotation of the Ni segment around the nanowire axis under the magnetic field (created by coupling a rotating magnet (A) and a static one (B); SI Scheme 1B). The magnetic field generates torques which leads to the rotation of the entire nanowire along its axis, resulting in breakage of the symmetry which induces the movement.

Tailoring the length of the Au 'head' and Ni 'tail' changes the asymmetry geometry and allows reversal of the motion direction. Different rotation amplitudes can thus be generated on both sides (Figure 1A(c) and B(c)), leading to the forward ('pusher') or backward ('puller') locomotion.^{3a} For example, flexible nanowires, with a longer Au segment ($3 \mu\text{m}$) and a shorter Ni one ($0.5 \mu\text{m}$), will move 'forward' in the rotating magnetic field (Figure 1A(b); SI Video 2). Under this condition, the rotation amplitude of the Ni segment (R_1) is much larger than the rotational amplitude of the Au segment (R_2), i.e. $R_1 \gg R_2$ (Figure 1A(c)), resembling a 'pusher'.^{3a} Here, the rotation of the Ni segment induces a flow field directed away from the nanowire along its swimming direction. The shorter the tail, the larger the conical angle of the nickel segment (compared to the gold one), and hence the larger the average force in the direction of the head (as the force and speed are directly proportional to the projection of the area in the direction of motion). Another factor that affects the motion is the fluid flow, which is moving at a higher speed relative to the swimmer on the lagging section. On the other hand, a 'backward' movement (with the Ni tail upfront) is observed with a shorter Au segment ($2 \mu\text{m}$) and a longer Ni one ($1 \mu\text{m}$). Such directed 'backward' (pulling) movement at a speed of $4 \mu\text{m s}^{-1}$ is illustrated in Figure 1B(b). Analogous experiments without dissolving the Ag segment display no directed movement (Figure 1B(a)). Additional data indicate that the 'backward' ('puller') motion is more efficient and offers higher reproducibility along with improved

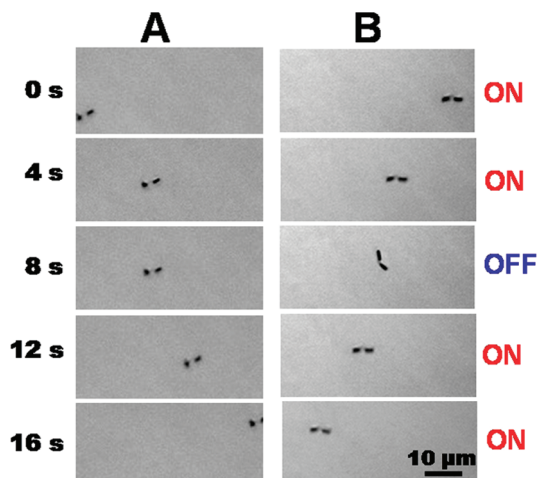


Figure 2. Time-lapse images illustrating the On/Off 'forward' (A) and 'backward' (B) motions of Au/Ag_{flex}/Ni nanomotors under the rotating magnetic field. Conditions are same as those in Figure 1. The images were taken every 4 s from SI Video 3.

motion control compared to the 'forward' one. This is in agreement with an early report comparing 'pullers' and 'pushers'.¹² This is also not surprising, as a pulling motion of slender bodies in a resistant medium is more stable than a pushing one (analogous to pushing a string on a frictional surface, as opposed to pulling it). Accordingly, such 'backward' motion was used in most subsequent work. Certain lengths of the 'tail' and 'head' (around 0.7 and $2.5 \mu\text{m}$, respectively) represent the crossover values where both 'forward' and 'backward' motions can be observed randomly.

Modulating the magnetic field allows precise On/Off motion control of the flexible nanowire motors. The magnetic nanowire motor stops and resumes its motion reversibly upon turning the magnetic field Off and On, respectively. For example, Figure 2 and the corresponding video (SI Video 3) demonstrate an On/Off/On cycle in connection to a modulated magnetic field, along with 'forward' (A) and 'backward' (B) movements. These data clearly illustrate that the directional movement of these nanomotors is stopped in the absence of the magnetic field and renewed upon switching the field 'On'. Note (from the video) that an initial rotation of the Ni 'tail' is essential for resuming the motion. Such precise motion control, along with other capabilities (described below), holds great promise for designing functional devices that perform multiple tasks. The flexible silver joint is highly rigid and does not break apart even under continuous prolonged operation in a rotating magnetic field with higher frequency and induction.

Our observations indicate that these magnetic swimmers display predictable and controllable behavior in the linear regime. For example, the nanomotor speed can be controlled by varying the frequency of the applied field. SI Figure 3 examines the dependence of the speed upon the frequency of the rotating magnetic field (5 G) over the 0–15 Hz range. The nanomotor speed increases from 1.5 to $6 \mu\text{m s}^{-1}$ upon raising the frequency from 5 to 15 Hz. Only Brownian motion was observed without applying the magnetic field.

Common catalytic nanowire motors operate only in low ionic-strength aqueous solutions,¹³ and hence cannot be applied in realistic biological environments. The magnetic nanowire swimmer addresses this ionic-strength limitation and can expand the scope of artificial nanomotors to salt-rich environments. SI Figure 4 and SI Video 4 compare the movement of the flexible nanowire in the absence of salt (a) and in 30 μM (b) and 30 mM (c) KCl solutions. These data indicate that the high ionic-strength medium has a

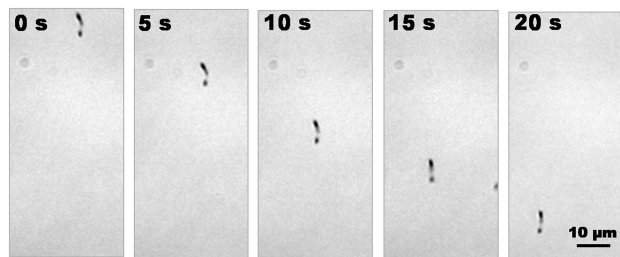


Figure 3. Time-lapse images of the ‘backward’ motion of Au/Ag_{flex}/Ni nanomotors in a urine sample under the rotating magnetic field. Conditions same as those in Figure 1B.

minimal effect upon the movement of the magnetic swimmers, with no obvious speed change in the different salt environments. The favorable locomotion in salt-rich environments has important implications upon future applications of artificial nanomotors. For example, Figure 3 displays time-lapse images of the movement of a magnetic nanowire swimmer in an undiluted urine sample. As indicated from the corresponding video (SI Video 5) the motor displays an efficient locomotion over a defined path in this biological medium.

In conclusion, we have demonstrated for the first time the propulsion of readily prepared flexible magnetic nanowire swimmers under an external magnetic field. Such magnetically driven nanowire locomotion obviates the fuel requirement of catalytic nanowire motors and resembles microorganisms that use a rotation mechanism for their motion. The simple design obviates also the requirement for helical (cork-screw) microstructures of recently described magnetic swimmers.^{6,7} Critical to the realization of such magnetic propulsion of nanowires is the flexibility of the Ag joint created by partial dissolution in hydrogen peroxide. The new magnetic nanomotors are mass produced using the template

electrodeposition strategy and could be functionalized (by modification of their Au segment) toward the creation of nanomachines performing practical tasks and diverse applications. In particular, the fuel-free operation could facilitate different biomedical applications such as targeted drug delivery.

Acknowledgment. This work was supported by NSF (Award Number CBET 0853375).

Supporting Information Available: Related protocols, instrumentation, reagents, additional data, and videos. This material is available free of charge via the Internet at <http://pubs.acs.org>.

References

- (1) (a) Mallouk, T. E.; Sen, A. *Sci. Am.* **2009**, *300*, 72–77. (b) Wang, J. *ACS Nano* **2009**, *3*, 4–9. (c) Mirkovic, T.; Zacharia, N. S.; Scholes, G. D.; Ozin, G. A. *ACS Nano* **2010**, *4*, 1782–1789.
- (2) Calvo-Marzal, P.; Sattayasamitsathit, S.; Balasubramanian, S.; Windmiller, J. R.; Dao, C.; Wang, J. *Chem. Commun.* **2010**, *46*, 1623–1624.
- (3) (a) Lauga, E.; Powers, T. R. *Rep. Prog. Phys.* **2009**, *72*, 096601. (b) Silverman, M.; Simon, M. *Nature* **1974**, *249*, 73–74.
- (4) Purcell, E. M. *Am. J. Phys.* **1977**, *45*, 3–11.
- (5) Dreyfus, R.; Baudry, J.; Roper, M. L.; Ferminger, M.; Stone, H. A.; Bibette, J. *Nature* **2005**, *437*, 862–865.
- (6) Zhang, L.; Abbott, J. J.; Dong, L. X.; Kratochvil, B. E.; Bell, D.; Nelson, B. J. *Appl. Phys. Lett.* **2009**, *94*, 64107.
- (7) Ghosh, A.; Fischer, P. *Nano Lett.* **2009**, *9*, 2243–2245.
- (8) (a) Geranio, L.; Heuberger, M.; Nowack, B. *Environ. Sci. Technol.* **2009**, *43*, 8113–8118. (b) Sun, X. M.; Li, Y. D. *Adv. Mater.* **2005**, *17*, 2626–2630.
- (9) Mirkovic, T.; Foo, M. L.; Arsenault, A. C.; Fournier-Bidoz, S.; Zacharia, N. S.; Ozin, G. A. *Nat. Nanotechnol.* **2007**, *2*, 565–569.
- (10) (a) Goszner, K.; Korner, D.; Hite, R. J. *Catal.* **1972**, *25*, 245–253. (b) Goszner, K.; Bischof, H. J. *Catal.* **1974**, *32*, 175–182.
- (11) Zhang, Q.; Cobley, C. M.; Zeng, J.; Wen, L.-P.; Chen, J.; Xia, Y. J. *Phys. Chem. C* **2010**, *114*, 6396–6400.
- (12) Hatwalne, H.; Ramaswamy, S.; Rao, M.; Simha, R. A. *Phys. Rev. Lett.* **2004**, *92*, 118101.
- (13) Paxton, W. F.; Baker, P. T.; Kline, T. R.; Wang, Y.; Mallouk, T. E.; Sen, A. *J. Am. Chem. Soc.* **2006**, *128*, 14881–14888.

JA1072349